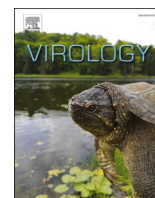




Since January 2020 Elsevier has created a COVID-19 resource centre with free information in English and Mandarin on the novel coronavirus COVID-19. The COVID-19 resource centre is hosted on Elsevier Connect, the company's public news and information website.

Elsevier hereby grants permission to make all its COVID-19-related research that is available on the COVID-19 resource centre - including this research content - immediately available in PubMed Central and other publicly funded repositories, such as the WHO COVID database with rights for unrestricted research re-use and analyses in any form or by any means with acknowledgement of the original source. These permissions are granted for free by Elsevier for as long as the COVID-19 resource centre remains active.



## Programmed –1 Ribosomal Frameshifting in coronaviruses: A therapeutic target

Jamie A. Kelly<sup>a</sup>, Michael T. Woodside<sup>b</sup>, Jonathan D. Dinman<sup>a,\*</sup>

<sup>a</sup> Department of Cell Biology and Molecular Genetics, University of Maryland, College Park, MD, 20742, USA

<sup>b</sup> Department of Physics, University of Alberta, Edmonton, AB, T6G 2E1, Canada

### ARTICLE INFO

#### Keywords:

Virus  
Coronavirus  
SARS-CoV  
SARS-CoV-2  
Covid-19  
Frameshifting  
Ribosome  
Antiviral  
Vaccine  
Therapeutics

### ABSTRACT

Human population growth, climate change, and globalization are accelerating the emergence of novel pathogenic viruses. In the past two decades alone, three such members of the coronavirus family have posed serious threats, spurring intense efforts to understand their biology as a way to identify targetable vulnerabilities. Coronaviruses use a programmed –1 ribosomal frameshift (–1 PRF) mechanism to direct synthesis of their replicase proteins. This is a critical switch in their replication program that can be therapeutically targeted. Here, we discuss how nearly half a century of research into –1 PRF have provided insight into the virological importance of –1 PRF, the molecular mechanisms that drive it, and approaches that can be used to manipulate it towards therapeutic outcomes with particular emphasis on SARS-CoV-2.

**Emerging viruses: the confluence of human population growth, globalization, and climate change.** Within the past generation, three interrelated but independent forces have driven the emergence of novel viral pathogens in the human population. Population growth has pushed humans into new ecosystems, increasing the number of contacts with zoonotic viruses, and hence the frequency of their adaptation to the new, human host (Karesh et al., 2012). Changes to ecosystems driven by climate change are altering the ranges of viral host species, enhancing the number of interspecies contacts (Mills et al., 2010). Lastly, economic globalization during this time period has created the means for the rapid, worldwide dissemination of novel pathogens (Sakar et al., 2004). As a result, we are witnessing an alarming increase in the number and frequency of novel viral epidemics. These include: the introduction of West Nile into North America in 1999 (Hadfield et al., 2019); the Severe Acute Respiratory Syndrome (SARS) near-pandemic of 2002–2003, and the narrowly averted breakout of the closely related Middle East Respiratory Syndrome Coronavirus (MERS-CoV) in 2012 (Xie and Chen, 2020); a similarly arrested Ebola threat in 2013–16 (Holmes et al., 2016); the emergence of Zika and Chikungunya virus in the Americas in 2015–16 (Weaver et al., 2018). Although a combination of sound policy and luck mitigated the impacts of these prior outbreaks, the ongoing COVID-19 crisis confirms the grim reality that emerging novel viral

pathogens will continue to pose one of the defining challenges of the 21st century.

**The coronavirus three step genetic program.** In humans, coronaviruses have traditionally been associated with causing approximately 10–30% of “common colds” (Paules et al., 2020). The perception of coronaviruses as relatively benign was dramatically altered with the emergence of SARS-CoV, and was further reinforced by MERS-CoV (Cui et al., 2019). As discussed elsewhere in this issue, these viruses are thought to be endemic in bats (Wong et al., 2019), and have moved to humans through intermediate species such as camels and exotic food animals in the context of crowded, unsanitary marketplaces (Volpato et al., 2020).

Similar to other betacoronaviruses, SARS-CoV-2 has a plus-sense RNA genome that is roughly 30 kb in length (Wu et al., 2020). The genome contains at least nine different open reading frames (ORFs), where ORF1a and ORF1b comprise of about two-thirds of the genome (Wang et al., 2020). The organization of the betacoronavirus genome reveals the viral developmental program (Fig. 1A). Upon entering a cell, the viral genomic RNA (gRNA) is released into the cytoplasm, where it functions as an mRNA. Since ORF1a is located at the 5' end of the gRNA, it is decoded first. ORF1a encodes proteins whose functions are to hijack the host cell by 1) securing the ribosomes, 2)

\* Corresponding author.

E-mail address: [dinman@umd.edu](mailto:dinman@umd.edu) (J.D. Dinman).

<https://doi.org/10.1016/j.virol.2020.12.010>

Received 9 October 2020; Received in revised form 15 December 2020; Accepted 16 December 2020

Available online 25 December 2020

0042-6822/© 2021 Elsevier Inc. This article is made available under the Elsevier license (<http://www.elsevier.com/open-access/userlicense/1.0/>).

disregulating the host cellular innate immune response, and 3) cleaving polyproteins into individual proteins. For example, nsp 1 hijacks the ribosomes by binding to the small subunit and occluding the mRNA entrance tunnel (Schubert et al., 2020). How this interaction favors translation of the viral mRNA remains unanswered, but the 5' untranslated region of the gRNA stimulates translation *in vitro*, suggesting that it contains a *cis*-acting element to bypass this block (Schubert et al., 2020), thus enabling the viral RNAs to “own” the ribosomes. Nsp 2 binds to prohibitin 1 and 2 and modulates host survival signaling in apoptosis (Cornillez-Ty et al., 2009). In addition to its ability to counteract host innate immunity through its ability to de-ADP-ribosylate, de-ubiquitinate, and remove Interferon stimulated gene 15 (ISG15) modifications from cellular proteins (i.e. de-ISGylate), nsp 3 also has papain-like protease activity which the virus uses to cleave the ORF1a and ORF1b polyproteins (Lei et al., 2018). Nsp 4 and nsp 6 function during the viral replication process to help the virus evade innate immune recognition (Angelini et al., 2013). ORF1b encodes proteins including the nsp 12 RNA-Dependent RNA polymerase (RDRP), the nsp 13 helicase, and the nsp 14/16 capping complex that are involved in the second stage of the viral replication program: RNA synthesis (Amor et al., 2020). Specifically, these proteins direct the synthesis of the (–) strand antigenome, which serves as a template for production of new capped, (+) strand gRNAs and the subgenomic RNAs (sgRNAs), whose ORFs are located in the 3'-most third of the viral genome. The sgRNAs encode mostly structural proteins, which defines the third step of the viral replication program, synthesis of structural proteins and viral particle assembly. This process can be diagrammed as a software program flowchart (Fig. 1B).

Expression of ORF1b requires a programmed –1 ribosomal frameshift event. In coronavirus genomes, ORF1a and ORF1b partially overlap, where ORF1b is in the –1 reading frame relative to ORF1a (Fig. 1A). Embedded in this overlap region is a *cis*-acting RNA element that directs a fraction of elongating ribosomes to slip by one base in the 5' (–1) direction in a process called Programmed –1 Ribosomal Frameshifting (–1 PRF). Upon a –1 frameshift, ribosomes are able to continue translating the ORF1b encoded proteins, enabling progression of the viral replication cycle from Stage 1 to Stage 2 as diagrammed in Fig. 1. A typical –1 PRF signal is composed of three elements. From 5' → 3', these are a heptameric slippery sequence at which the slippage occurs, a short spacer, and a proximal downstream stimulatory structure in the mRNA that directs the ribosome to pause over the slippery site (Fig. 2A and B). The slippery site most often has the sequence N NNW WWH (the

incoming 0-frame is indicated by spaces), Where NNN = any three identical bases, WWW = three A's or three U's, and H ≠ G (Fig. 2B). With a few exceptions, the stimulatory structure is an RNA pseudoknot, in which the RNA strand folds back on itself one or more times to form a variety of complex but compact and stable structures (e.g., see Fig. 2C–E).

The molecular mechanisms underlying –1 PRF have been deeply investigated. The “simultaneous slippage” model of –1 PRF (Jacks et al., 1988) posits that the downstream stimulatory element makes elongating ribosomes pause with their A- and P-site tRNAs over the slippery site in the 0-frame. The nature of the tRNAs and slippery site are such that, upon a –1 slippage event, the tRNA non-wobble bases can re-pair to the –1 frame codons. The pseudoknot was first discovered in a coronavirus, Avian Infectious Bronchitis Virus (Brierley et al., 1989), and this system was subsequently used to demonstrate pseudoknot-induced ribosomal pausing over the –1 PRF signal (Somogyi et al., 1993). While the complete mechanism and structural biology underlying mRNA pseudoknot stimulation of recoding has not been fully elucidated, our current understanding is described as follows. The “torsional restraint” model (Plant and Dinman, 2005) proposes that, as an elongating ribosome begins to unwind Stem 1 of the pseudoknot, supercoiling in Stem 2 impedes the ribosomes' progress such that a point is reached where the forward motion of the ribosome is countered by the resistance of the pseudoknot to unwinding. This effect, in combination with a spacer of optimal length, serves to direct ribosomes to pause with their A- and P-sites at the slippery site. The “9 Å Solution” model of –1 PRF (Plant et al., 2003) was founded on atomic-resolution structural data indicating that the mRNA is pulled into the ribosome by one base during the process of aa-tRNA accommodation (Noller et al., 2002). In this model, the downstream stimulatory structure impedes this movement, stretching the segment of mRNA located between the slippery site and the stimulatory structure. The resulting local tension in the mRNA can be resolved either by unwinding the stimulatory structure or by slippage into the –1 frame. A similar mechanism can also be applied to co-translocational –1 PRF events (Bock et al., 2019; Caliskan et al., 2014, 2017; Chen et al., 2014; Kim et al., 2014). An important feature of this model is that the energy provided by the GTPase power stroke of either eEF1A or eEF2 is sufficient to drive tRNA unpairing from the 0-frame codons, a critical prerequisite for –1 PRF (Bock et al., 2019; Caliskan et al., 2014; Plant et al., 2003; Rodnina et al., 1995). Additional structural and kinetic analyses using purified *E. coli* ribosomes and elongation factors have shown that the downstream pseudoknot in the mRNA can impede the

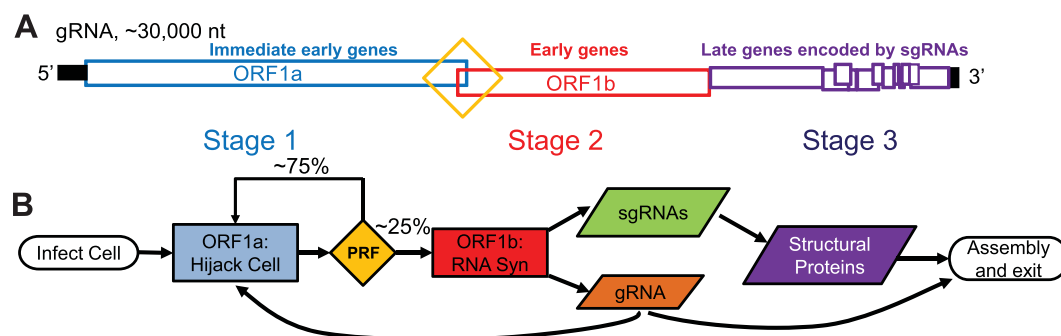


**Fig. 1.** Betacoronavirus gene organization and expression flowchart. A. Map of the betacoronavirus genomic RNA (gRNA). Open reading frames are color-coded and the –1 PRF signal is indicated inside of the yellow diamond. B. Flowchart of the intracellular coronavirus (CoV) replication program. Upon infection and release of viral genomic RNA into the cytoplasm, ORF1a-encoded proteins are synthesized first, initiating Stage 1 of the program. Their function is to “hijack” the cell by securing the ribosomes and disrupting the host cellular innate immune response. Approximately one quarter of translating ribosomes are induced to shift reading frame at the –1 PRF signal. This –1 PRF signal represents a decision point: to continue with Stage 1 or to move into Stage 2, wherein proteins expressed from ORF1b are synthesized in order to transcribe new viral RNAs, including new genomic and subgenomic RNAs. New gRNAs also provide feedback to reinforce cellular takeover by the virus. The transition to Stage 2 may either be rapid, requiring the accumulation of a critical mass of ORF1b products to generate a rapid burst of RNA synthesis (e.g. the rate of viral factory assembly may be determined by –1 PRF rates), or it may be a gradual process instead. In Stage 3, structural proteins encoded in the subgenomic RNAs package the genomic RNAs to produce new viral particles, which exit to repeat the infectious cycle. (For interpretation of the references to color in this figure legend, the reader is referred to the Web version of this article.)

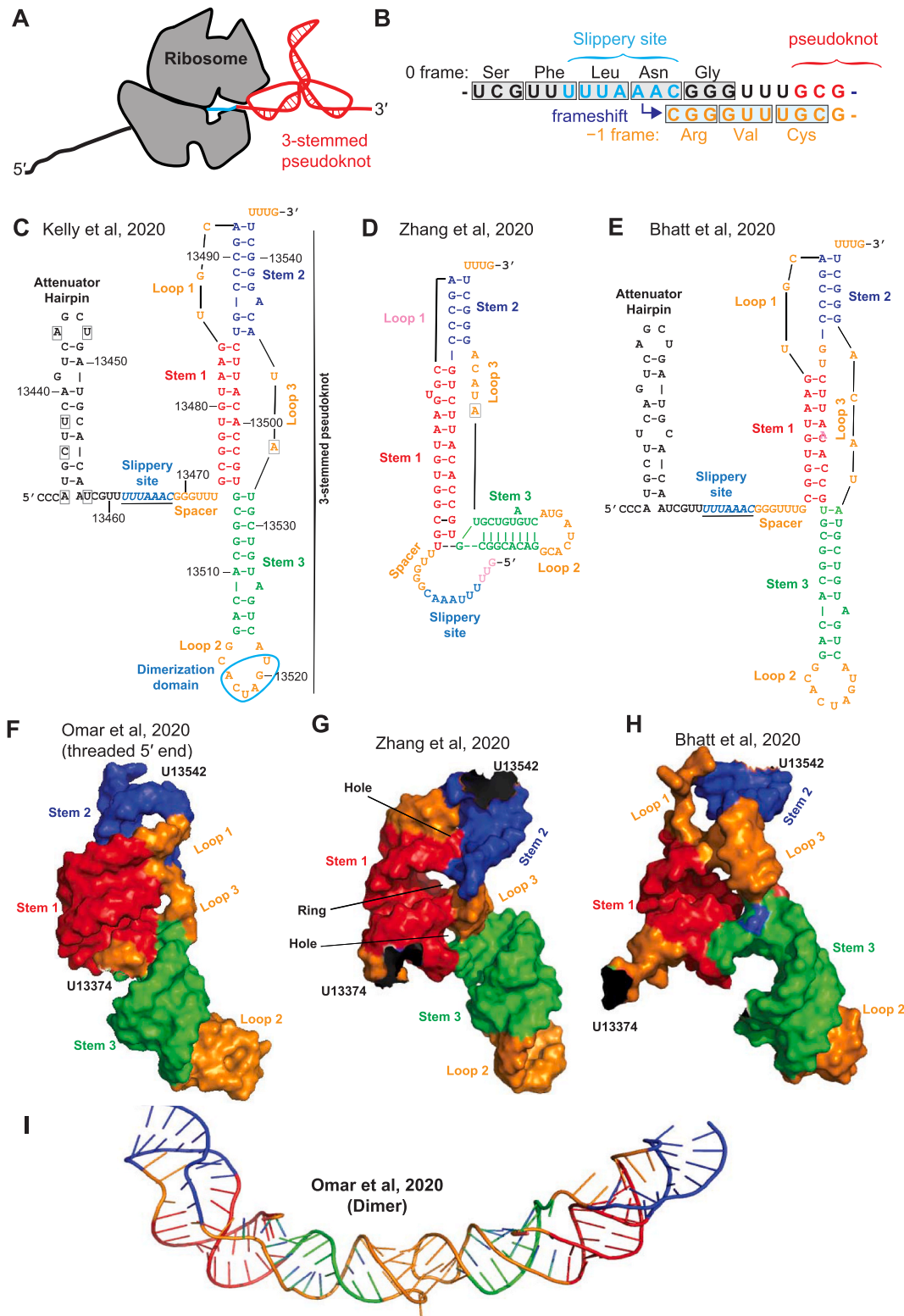


**Fig. 2.** –1 PRF in SARS-CoV and SARS-CoV-2. A-B. Cartoon showing elements involved in –1 PRF and example of shift in reading frame. Elongating ribosomes pause at the 3-stemmed pseudoknot with A- and P-site tRNAs base-paired respectively to AAG and UUA codons in slippery site; upon slippage, non-wobble bases of tRNAs can re-pair to –1 frame codons AAA and UUU. C-E. Comparison of the two-dimensional representations of the SARS-CoV-2 –1 PRF signals. Data from (Bhatt et al., 2020; Kelly et al., 2020; Zhang et al., 2020) are labeled and color-coded as indicated. The nucleotides that differ between SARS-CoV-2 and SARS-CoV are boxed in grey. The dimerization domain identified in (Ishimaru et al., 2013) is circled in cyan. F-H. Space-filling models of the SARS-CoV-2 three stemmed pseudoknot. From left to right, an example of a 5'-end threaded conformation generated by molecular dynamics simulations (Omar et al., 2020), the cryo-EM structure of an isolated pseudoknot (Zhang et al., 2020), and the cryo-EM image of the pseudoknot in the context of a paused ribosome (Bhatt et al., 2020). I. A model of the dimerized SARS-CoV-2 –1 PRF signal from molecular dynamics simulations (Omar et al., 2020). (For interpretation of the references to color in this figure legend, the reader is referred to the Web version of this article.)

closing movement of the large subunit head, arresting it in a hyper-rotated state, which delays dissociation of the translocase and the release of deacylated tRNA. Release of the tension on the mRNA by ribosomal slippage accelerates completion of translocation, providing a lower-energy path for the ribosome to continue translation (Chen et al., 2014; Rodnina et al., 2019; Yan et al., 2015). More recently, an endogenous cellular protein called Shiftless was identified that binds to frameshifted, hyper-rotated ribosomes, arresting their translation and promoting translation termination by recruiting the termination factors (Wang et al., 2019).

Whether downstream stimulatory structures play active roles in directing  $-1$  PRF remains an open question. It has been known for some time that thermodynamic stability corresponds with  $-1$  PRF efficiency, but only to a limited extent: pseudoknots that are too stable inhibit  $-1$  PRF, presumably because they cannot be resolved by translating ribosomes (Marczinke et al., 1998). Numerous studies suggest that dynamic mRNA structural remodeling is required for optimal  $-1$  PRF efficiency (Chen et al., 2013; Halma et al., 2019, 2020; Kendra et al., 2017; Kim et al., 2014; Moomau et al., 2016; Ritchie et al., 2012, 2014, 2017; Yang et al., 2018). Coordination of base triples in both major and minor grooves provides mechanical resistance to pseudoknot unwinding and stretches of adenosines confined along the minor groove of a helix also provide resistance. Together, these molecular features contribute to ribosome pausing at the slippery site to help stimulate  $-1$  PRF (Chen et al., 2017; Halma et al., 2019). Thus, while it was initially thought that downstream stimulatory structures were merely passive “roadblocks,” the most recent research suggests that they are actively involved. What ‘active’ means in this context remains an evolving question. For example, it may involve the deformation of one structure that strongly impedes ribosome progress, followed by structural remodeling to another conformer that does not, or it may be that fluctuations in the mRNA tension induced by conformational switching play a role in inducing slippage. Additionally, biophysical and mutational analyses revealed that the terminal loop (i.e., loop 2) of the SARS-CoV  $-1$  PRF stimulating pseudoknot mediates RNA dimerization and that this plays a role in determining  $-1$  PRF efficiency (Ishimaru et al., 2013). Notably, this sequence is conserved in SARS-CoV-2 (Fig. 2C and I) (Kelly et al., 2020). The role of dimerization in  $-1$  PRF remains unknown.

### 1. Structural biology: 3-stemmed RNA pseudoknots in coronavirus $-1$ PRF signals

There is strong phylogenetic, genetic, and biophysical evidence showing that the alpha- and betacoronaviruses share a common 3-stem fold, rather than the 2-stem structure typical of most stimulatory pseudoknots (Baranov et al., 2005; Harcourt et al., 2020; Omar et al., 2020; Plant et al., 2005; Ramos et al., 2004; Zhang et al., 2020) (Fig. 2C, D, 2E). This 3-stem architecture is highly conserved among betacoronaviruses (Rangan et al., 2020) but seems to be unique to the coronavirus family (Plant and Dinman, 2008). The SARS-CoV-2 pseudoknot is nearly identical in sequence to the SARS-CoV pseudoknot, differing only in having A instead of C at position 13,533 in loop 3. The results from structural probes of the SARS-CoV pseudoknot (Ishimaru et al., 2013; Plant et al., 2005, 2010) are thus likely to apply also to the SARS-CoV-2 pseudoknot. Indeed, small-angle X-ray scattering analyses of global morphology confirms that the SARS-CoV and SARS-CoV-2 pseudoknots occupy effectively identical space-filling envelopes (Kelly et al., 2020), and NMR spectra (Wacker et al., 2020) revealed a similar secondary structure to that deduced previously for the SARS-CoV pseudoknot from nuclease-protection assays (Plant et al., 2005), although with the end of stem 2 unpaired to extend loop 3. Based on the secondary structure from nuclease-protection assays, atomistic molecular dynamics simulations found an ensemble of possible structures with networks of tertiary contacts consistent with the resistance of the SARS-CoV pseudoknot to mechanical unfolding (Omar et al., 2020). Intriguingly, this ensemble encompasses different fold topologies,

including one with the 5' end threaded through the junction between stems 1 and 3 (Fig. 2F). The 5'-end threading creates an unusual “ring-knot” structure previously only seen in viral exoribonuclease-resistant RNAs (Akiyama et al., 2016).

Cryo-EM imaging of the SARS-CoV-2 pseudoknot confirms that it forms an ensemble of structures, with both rod-like and bent conformers observed, including some with a ring-like feature (Zhang et al., 2020). This 88-nt RNA is also notable for being the smallest biomolecule resolved by single-particle cryo-EM to date. A preliminary 5.9 Å resolution structure of the ring-like subpopulation reveals the presence of two “holes” in addition to the open ring (Fig. 2G), which may present small-molecule binding/docking sites. The ring provides space for threading of the 5' end, similar to what was seen in molecular dynamics modeling (Omar et al., 2020) (Fig. 2F), confirming the presence of this unusual topology. However, the base-pairing is different in this structure from the pairing deduced from nuclease-protection results (Plant et al., 2005) and NMR (Wacker et al., 2020), featuring an extended stem 1, loss of loop 1, shortened stem 2, and lengthened loop 3. As a result, none of the stems are stacked, unlike what is often seen in stimulatory pseudoknots. These differences may arise from the high  $Mg^{2+}$  concentration used for the imaging. This cryo-EM reconstruction also includes a mini-helix formed within the slippery site and spacer region upstream of the pseudoknot. However, RNA chemical modification studies of the SARS-CoV-2 genome reveal that the slippery site is single-stranded (Huston et al., 2020; Iserman et al., 2020; Lan et al., 2020; Manfredonia et al., 2020; Zhang et al., 2020), suggesting that the mini-helix is an artifact of the construct used for cryo-EM imaging.

A second cryo-EM study has imaged the SARS-CoV-2  $-1$  PRF signal not in isolation, but on an arrested mammalian ribosome that is primed for frameshifting (Bhatt et al., 2020) (Fig. 2H). In this  $\sim 2.3 - 7$  Å reconstruction, the RNA is positioned with its slippery-site codons in the 0-frame, a peptidyl-phenylalanyl tRNA base-paired to the ribosomal P-site, and the spacer region pulled into the mRNA entrance tunnel. It should be noted that in order to stall ribosomes at the  $-1$  PRF signal, the 0-frame A-site codon was changed from AAC to UAA and *in vitro* translation reactions were supplemented with an excess of a mutant eRF1 (AAQ) in order to trap ribosomes in the act of decoding the A-site. These non-rotated ribosomes thus represent a pre-frameshift complex, which necessarily limits what can be learned about the  $-1$  PRF process itself. Nonetheless, this structure presents a wealth of novel information. Consistent with the unwinding of the pseudoknot by the intrinsic ribosomal helicase (Rabl et al., 2011; Takyar et al., 2005), the spacer and stem 1 of the pseudoknot interact with basic residues in the C-terminal domain of ribosomal proteins uS5 and eS30. A direct interaction between helix 16 of the 18S rRNA and minor groove of stem 1 was also noted: this interaction may restrict the relative rotation between the head and body of the small subunit during translocation, which has been shown to be important for the  $-1$  PRF process (Caliskan et al., 2014). Similar to the structures described above, the 5' end is threaded through a ring formed by the junction between the 3 stems. Whereas the quasi-coaxial stacking of stems 1 and 2 resembles what is seen in the threaded structures described by Omar et al. the interaction of the  $-1$  PRF signal with the ribosome appears to have caused significant restructuring of this element (compare Fig. 2F and G with Fig. 2H). In particular, stem 1 is distorted towards the 5' end and shortened by 1 base-pair, loop 1 is less compact and breaks triples with stem 2 in favor of interactions with the ribosome, loop 3 is extended by shortening stem 2 but also loses tertiary contacts with stem 1, while stem 3 is lengthened by 1 base-pair and most notably is rotated nearly perpendicular to the axis formed by stems 1 and 2. These results suggest that the interaction of the pseudoknot with the ribosome results in significant restructuring of the frameshift-stimulating element, consistent with SAXS analyses (Kelly et al., 2020) and molecular dynamics simulations indicating the presence of a complex structural ensemble of conformers (Omar et al., 2020). These findings support an emerging theme wherein “shapeshifting” RNAs are important for regulating gene expression (Dinman, 2018, 2019a). Beyond well-documented examples

in mRNA splicing, others include the ability of different conformers of the nc886 RNA to control activation of RNase L and its ability to activate the immune response (Calderon and Conn, 2017), and the interactions of mRNAs with Argonaute (Ruijtenberg et al., 2020). Currently, small- and wide-angle x-ray scattering (SAXS and WAXS) (Kelly et al., 2020), single-molecule force spectroscopy (Halma et al., 2019), time-resolved cryo-EM (Frank, 2017), new biophysical assays of  $-1$  PRF including ribosome profiling (Belew et al., 2014) and nanopore-based applications (Zhang et al., 2015), and computational advances are being exploited to visualize and model the process of  $-1$  PRF.

## 2. Functional analyses of the SARS-CoV and SARS-CoV-2 $-1$ PRF signals

Historically, a series of molecular genetics and biochemical analyses of the Avian Infectious Bronchitis Virus  $-1$  PRF signal established the foundation for much of our understanding of this phenomenon (Brierley et al., 2007; Brierley and Pennell, 2001). Analyses of SARS-CoV-2 sequence variations reveal the highly conserved nature of the  $-1$  PRF signal; the vast majority of variants are very infrequently represented in the population, supporting the importance of this element for viral fitness (Ryder et al., 2020). Functional studies of single-nucleotide polymorphisms seen in different regions of the pseudoknot found that most of them had little effect on  $-1$  PRF efficiency (Neupane et al., 2020), with only a few leading to significant decreases, including a  $\sim 2$ -fold decrease from C13476U and C13501U in stem 1 (Sun et al., 2020) and a roughly 3-fold decrease from U13494C in stem 2 (Neupane et al., 2020); notably, each of these mutations involved converting G:C pairs to G:U (or vice versa), and hence would be expected to leave the secondary structure unchanged. Stems 1 and 2 of the SARS-CoV and SARS-CoV-2 pseudoknots are absolutely required to promote  $-1$  PRF, but stem 3 is not; rather it appears to function to further stimulate this activity (Baranov et al., 2005; Kelly et al., 2020; Plant et al., 2005, 2010). In loop 1, changing G13486 to A reduces  $-1$  PRF to roughly one-third of wild-type levels, while changing it to C reduced it even further (Bhatt et al., 2020); similarly, the U13485C mutation reduces  $-1$  PRF more than two-fold (Sun et al., 2020). Mutations to A13535 and A13537, located in loop 3 and/or stem 2 (depending on the structural model), also abrogated efficient  $-1$  PRF (Bhatt et al., 2020; Plant et al., 2005). These observations also support the idea that structural plasticity plays an important role in the  $-1$  PRF mechanism. Additionally, the placement of the 0-frame stop codon appears to play an important role in determining  $-1$  PRF efficiency, and a model has been proposed in which the process of termination by a leading ribosome provides the pseudoknot time to re-fold before a trailing ribosome encounters the  $-1$  PRF stimulating sequence (Bhatt et al., 2020).

The SARS-CoV and SARS-CoV-2  $-1$  PRF signals also harbor a novel “attenuator hairpin” element located immediately upstream of the slippery site (Cho et al., 2013; Su et al., 2005) (Fig. 2C and E). The attenuation model posits that the hairpin is initially unwound by an elongating ribosome as it approaches the frameshift signal. As it enters the slippery site, the ribosome clears the attenuator sequence, enabling the stem-loop to re-form. Its formation enables it to block the backwards slippage of the ribosome. While the primary sequence of the SARS-CoV-2 attenuator element is not as well conserved with its SARS-CoV counterpart as compared to their core  $-1$  PRF signals, both have been shown to have  $-1$  PRF-tempering activities (Kelly et al., 2020). Additionally, *in silico* analysis of the SARS-CoV-2 “structure” suggests that the  $-1$  PRF signal is nested inside of a larger, double-stranded RNA superstructural domain (Andrews et al., 2020).

## 3. $-1$ PRF as a critical developmental switch

As noted above, expression of the ORF1b proteins require a  $-1$  PRF event. From the programmatic point of view shown in Fig. 1B,  $-1$  PRF

represents a decision nexus: either remain in Stage 1 of the infectious program or progress to Stage 2. Notably,  $-1$  PRF does not happen with 100% efficiency; rather,  $-1$  PRF directed by the SARS-CoV and SARS-CoV-2 elements occur at an efficiency of  $\sim 15$ – $30\%$ , depending on the assay system (Bhatt et al., 2020; Kelly et al., 2020; Plant et al., 2005). In viruses such as HIV-1,  $-1$  PRF rates determine the ratio of structural (e. g. the Gag polyprotein) to enzymatic proteins (the Gag-pol polyprotein), and the prevailing model is that the rate of  $-1$  PRF ensures the production of the correct ratios of structural to non-structural proteins (Dever et al., 2018). However, this situation does not apply to coronaviruses because the ORF1a proteins do not encode structural proteins. Instead, we suggest that  $-1$  PRF in these viruses may have a timing function. We propose that by delaying the accumulation of the RNA replication machinery until some critical concentration is reached—which could be important for building a viral factory (Neuman et al., 2014), for example, a process that may involve a concentration-dependent phase transition of the viral replication complex (Galloux et al., 2020; Zhou et al., 2019)—the virus may buy time for the ORF1a-encoded non-structural proteins to amass to high enough concentrations that they can incapacitate the host cell’s innate immune response. This time delay may be important because of the transient production of dsRNAs during the RNA replicative phase, which may activate various arms of the innate immune response (Maillard et al., 2019). From a biochemical/biophysical vantage point, slowing the buildup of viral replicase may maximize the timing at which a critical concentration of this enzyme is achieved, enabling a burst of RNA synthesis at the right time during the viral replication cycle.

## 4. $-1$ PRF is a novel target for antiviral therapeutics

An early study of  $-1$  PRF in a totivirus demonstrated that the native rate of frameshifting produced the correct stoichiometric ratios of structural to enzymatic viral proteins, and that either increasing or decreasing  $-1$  PRF efficiencies inhibited viral replication (Dinman and Wickner, 1992). Consistent with this model, overexpression of retroviral Gag-pol protein inhibited viral replication (Karacostas et al., 1993). Later studies revealed that  $-1$  PRF rates can also be altered by small molecules to interfere with viral replication, thereby identifying  $-1$  PRF as a potential therapeutic target (Dinman et al., 1997; Goss Kinzy et al., 2002). These findings were later extended to the SARS-CoV  $-1$  PRF signal, showing that mutants (Plant et al., 2010, 2013), antisense peptide nucleic acids (Ahn et al., 2011), and a small-molecule inhibitor of  $-1$  PRF, 2-methylthiazol-4-ylmethyl-[1,4]diazepane-1-carbonyl]amino}benzoic acid ethyl ester (MDTB) (Park et al., 2011), all negatively impacted virus replication. The  $-1$  PRF signals of the SARS-CoV family may be particularly good drug targets because a) there is no known case of  $-1$  PRF promoted by a three-stemmed pseudoknot structure in host cellular mRNAs; b) the  $-1$  PRF signal is highly conserved because it has to maintain structure while coding for two overlapping genes, and thus it is not likely to mutate to evade drug interactions; and c) the structure of the pseudoknot is sufficiently complex to contain well-defined binding pockets, with the 5'-end threading in particular generating a unique pocket geometry. This notion has elicited a burst of recent research aimed at identifying small molecules that target the SARS-CoV-2  $-1$  PRF signal (Manfredonia et al., 2020). For example, MDTB was also shown to inhibit SARS-CoV-2  $-1$  PRF (Kelly et al., 2020) and viral replication (Bhatt et al., 2020). Similarly, this agent appears to be resistant to natural variants of the SARS-CoV-2  $-1$  PRF stimulating pseudoknot (Neupane et al., 2020). A recent screen of a bank of approved drugs identified numerous small molecules that either stimulated or inhibited SARS-CoV-2 mediated  $-1$  PRF (Chen et al., 2020). Independently, another group identified merafloxacin, a fluoroquinolone antibacterial, as a potent inhibitor of SARS-CoV-2  $-1$  PRF and viral replication in Vero-E6 cells, which also showed resistance to natural mutations and activity against other human betacoronaviruses (Sun et al., 2020). We have also identified numerous small-molecule inhibitors (Dinman, unpublished). Although there does

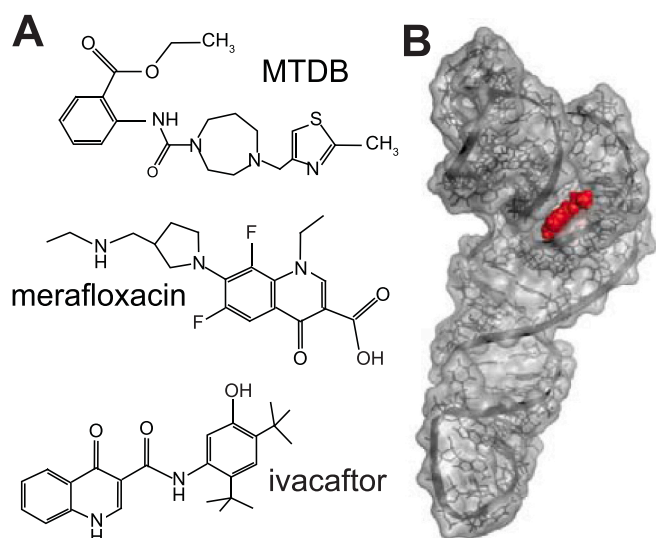


**Fig. 3.** Small-molecule inhibitors of  $-1$  PRF in SARS-CoV-2. **A.** Three examples of small molecules that have been found to inhibit  $-1$  PRF: MTDB (Kelly et al., 2020), merafloxacin (Sun et al., 2020), and ivacaftor (Chen et al., 2020). **B.** Binding site of MTDB on SARS-CoV-2 pseudoknot. Model of the binding site of MTDB (red) found from docking calculations and molecular dynamics simulations of the bound complex shows the ligand binds in a cleft formed because of 5'-end threading in the pseudoknot. (For interpretation of the references to color in this figure legend, the reader is referred to the Web version of this article.)

not appear to be overlap among all of the screens reported to date, the compounds identified thus far are rich in hydrophobic cyclic structures (Fig. 3A), suggesting that they may bind to the “ring” and “holes” identified by molecular dynamics simulations (Omar et al., 2020) and cryo-EM (Zhang et al., 2020). Indeed, computational modeling of the binding of MTDB to the SARS-CoV (Park et al., 2011) and SARS-CoV-2 (Woodside, unpublished) pseudoknots shows that it binds to a cleft formed by the threading of the 5' end (Fig. 3B). Intriguingly, interactions with the pseudoknot alone are insufficient to explain the inhibitory effect of MTDB, since its  $K_d$  of  $\sim 200$   $\mu\text{M}$  for pseudoknot binding (Ritchie et al., 2014) is many times higher than  $\text{IC}_{50}$  for suppressing  $-1$  PRF (Kelly et al., 2020; Park et al., 2011) or viral replication (Bhatt et al., 2020), suggesting that its binding is enhanced by the presence of ribosomes, for example owing to direct contacts with the ribosome or effects from ribosome-induced remodeling of the pseudoknot. It remains unclear to what extent similar considerations may apply to other small-molecule inhibitors. In parallel to exploration of small-molecule inhibitors, antisense targeting of the  $-1$  PRF signal is also being explored as a therapeutic approach (Plant et al., 2013; Zhang et al., 2020).

The  $-1$  PRF attenuator hairpin also presents a target for antiviral intervention. For example, annealing of an antisense RNA or DNA oligonucleotide to upstream of the MERS-CoV  $-1$  PRF signal strongly inhibited frameshifting (Hu et al., 2016). Similarly, a drug-like small molecule has been identified that binds with high affinity to the SARS-CoV-2 frameshift-attenuator hairpin, stabilizing it in its folded state and attenuating  $-1$  PRF in a cell-based assay (Haniff et al., 2020). Additionally, when ligated to RIBOTAC, a ribonuclease targeting chimera, it can recruit a cellular protease to degrade the viral RNA.

An alternative approach to small-molecule or anti-sense inhibitors may be to develop attenuated viral vaccine strains that incorporate mutated  $-1$  PRF signals. These RNA elements may be particularly amenable to such an approach because multiple silent coding mutations can be incorporated into the slippery-site and pseudoknot-forming regions, thus decreasing the chances of mutational reversion. For example, mutations of the slippery site of Venezuelan Equine Encephalitis Virus that promoted decreased rates of  $-1$  PRF only mildly delayed the

kinetics of VEEV accumulation in cultured cells, but strongly inhibited its pathogenesis in an aerosol infection mouse model, including decreasing viral titers in the brain (Kendra et al., 2017). Preliminary data indicate that mice infected with this mutant are protected from subsequent challenge with a highly pathogenic version of the virus (Dinman and Kehn-Hall, unpublished). These findings suggest a novel approach to the development of safe and effective live attenuated vaccines directed against  $-1$  PRF-utilizing viruses, including members of the SARS-like coronaviruses. As a final thought, it may be possible to exploit the  $-1$  PRF inhibitor Shiftless as a means to control viral infection (Dinman, 2019b).

## Funding

This work was supported by Defense Threat Reduction Agency Grant HDTRA1-13-1-0005 and a University of Maryland Coronavirus Research Program Seed Grant to JDD, and Canadian Institutes of Health Research grant OV3-170709 to MTW. JAK was supported by training grant from the NIH to the University of Maryland Graduate Program in Virology (2T32AI051967-06A1).

## CRediT authorship contribution statement

**Jamie A. Kelly:** All authors contributed equally to the writing and editing of this work. **Michael T. Woodside:** All authors contributed equally to the writing and editing of this work. **Jonathan D. Dinman:** All authors contributed equally to the writing and editing of this work.

## Declaration of competing interest

The authors declare that they have no conflicts of interest with the contents of this article.

## Acknowledgements

We wish to thank members of the Dinman lab, both past and present for their efforts investigating the SARS-CoV and SARS-CoV-2  $-1$  PRF signals, with special thanks to Dr. Ewan Plant. We also thank Drs. Lois Pollack, Kyle Kehn-Hall, and Nenad Ban for their strong collaborative spirit and sharing of preliminary information. JDD extends his heartfelt thanks to the doctors, nurses and staff of the Covid-19 ward at Suburban Hospital in Bethesda MD for their wonderful care.

## References

- Ahn, D.G., Lee, W., Choi, J.K., Kim, S.J., Plant, E.P., Almazan, F., Taylor, D.R., Enjuanes, L., Oh, J.W., 2011. Interference of ribosomal frameshifting by antisense peptide nucleic acids suppresses SARS coronavirus replication. *Antivir. Res.* 91, 1–10.
- Akiyama, B.M., Laurence, H.M., Massey, A.R., Costantino, D.A., Xie, X., Yang, Y., Shi, P. Y., Nix, J.C., Beckham, J.D., Kieft, J.S., 2016. Zika virus produces noncoding RNAs using a multi-pseudoknot structure that confounds a cellular exonuclease. *Science* 354 (80), 1148–1152. <https://doi.org/10.1126/science.aah3963>.
- Amor, S., Fernández Blanco, L., Baker, D., 2020. Innate immunity during SARS-CoV-2: evasion strategies and activation trigger hypoxia and vascular damage. *Clin. Exp. Immunol.* 202, 193–209. <https://doi.org/10.1111/cei.13523>.
- Andrews, R., Peterson, J., Haniff, H., Chen, J., Williams, C., Grefe, M., Disney, M., Moss, W., 2020. An in silico map of the SARS-CoV-2 RNA Structureome. *bioRxiv Prepr. Serv. Biol.* <https://doi.org/10.1101/2020.04.17.045161>.
- Angelini, M.M., Akhlaghpour, M., Neuman, B.W., Buchmeier, M.J., 2013. Severe acute respiratory syndrome coronavirus nonstructural proteins 3, 4, and 6 induce double-membrane vesicles. *mBio* 4. <https://doi.org/10.1128/mBio.00524-13>.
- Baranov, P.V., Henderson, C.M., Anderson, C.B., Gesteland, R.F., Atkins, J.F., Howard, M.T., 2005. Programmed ribosomal frameshifting in decoding the SARS-CoV genome. *Virology* 332, 498–510.
- Belew, A.T., Meskauskas, A., Musalgaonkar, S., Advani, V.M., Sulima, S.O., Kasprzak, W., Shapiro, B.A., Dinman, J.D., 2014. Ribosomal frameshifting in the CCR5 mRNA is regulated by miRNAs and the NMD pathway. *Nature* 512, 265–269. <https://doi.org/10.1038/nature13429>.
- Bhatt, P.R., Scaiola, A., Loughran, G., Leibundgut, M., Kratzel, A., McMillan, A., O, K.M., Bode, J.W., Thiel, V., Atkins, J.F., Ban, N., 2020. Structural basis of ribosomal

- frameshifting during translation of the SARS-CoV-2 RNA genome. *bioRxiv* 10 (26), 355099. <https://doi.org/10.1101/2020.10.26.355099>, 2020.
- Bock, L.V., Caliskan, N., Korniy, N., Peske, F., Rodnina, M.V., Grubmüller, H., 2019. Thermodynamic control of -1 programmed ribosomal frameshifting. *Nat. Commun.* 10, 4598. <https://doi.org/10.1038/s41467-019-12648-x>.
- Brierley, I., Pennell, S., 2001. Structure and function of the stimulatory RNAs involved in programmed eukaryotic-1 ribosomal frameshifting. *Cold Spring Harbor Symp. Quant. Biol.* 66 (233–48), 233–248.
- Brierley, I., Pennell, S., Gilbert, R.J., 2007. Viral RNA pseudoknots: versatile motifs in gene expression and replication. *Nat. Rev. Microbiol.* 5, 598–610.
- Brierley, I.A., Dingard, P., Inglis, S.C., 1989. Characterization of an efficient coronavirus ribosomal frameshifting signal: requirement for an RNA pseudoknot. *Cell* 57, 537–547.
- Calderon, B.M., Conn, G.L., 2017. Human noncoding RNA 886 (nc886) adopts two structurally distinct conformers that are functionally opposing regulators of PKR. *RNA* 23, 557–566. <https://doi.org/10.1261/rna.060269.116>.
- Caliskan, N., Katunin, V.I., Belardinelli, R., Peske, F., Rodnina, M.V., 2014. Programmed -1 frameshifting by kinetic partitioning during impeded translocation. *Cell* 157, 1619–1631. <https://doi.org/10.1016/j.cell.2014.04.041>.
- Caliskan, N., Wohlgemuth, I., Korniy, N., Pearson, M., Peske, F., Rodnina, M.V., 2017. Conditional switch between frameshifting regimes upon translation of dnaX mRNA. *Mol. Cell* 66, 558–567. <https://doi.org/10.1016/j.molcel.2017.04.023> e4.
- Chen, J., Petrov, A., Johansson, M., Tsai, A., O'Leary, S.E., Puglisi, J.D., O'Leary, S.E., Puglisi, J.D., 2014. Dynamic pathways of -1 translational frameshifting. *Nature* 512, 328–332. <https://doi.org/10.1038/nature13428>.
- Chen, J., Petrov, A., Tsai, A., O'Leary, S.E., Puglisi, J.D., 2013. Coordinated conformational and compositional dynamics drive ribosome translocation. *Nat. Struct. Mol. Biol.* 20, 718–727.
- Chen, Y.-T., Chang, K.-C., Hu, H.-T., Chen, Y.-L., Lin, Y.-H., Hsu, C.-F., Chang, C.-F., Chang, K.-Y., Wen, J.-D., 2017. Coordination among tertiary base pairs results in an efficient frameshift-stimulating RNA pseudoknot. *Nucleic Acids Res.* 45, 6011–6022. <https://doi.org/10.1093/nar/gkx134>.
- Chen, Y., Tao, H., Shen, S., Miao, Z., Li, L., Jia, Y., Zhang, H., Bai, X., Fu, X., 2020. A drug screening toolkit based on the -1 ribosomal frameshifting of SARS-CoV-2. *Heliyon* 6. <https://doi.org/10.1016/j.heliyon.2020.e04793>.
- Cho, C.-P., Lin, S.-C., Chou, M.-Y., Hsu, H.-T., Chang, K.-Y., 2013. Regulation of programmed ribosomal frameshifting by co-translational refolding RNA hairpins. *PLoS One* 8, e62283. <https://doi.org/10.1371/journal.pone.0062283>.
- Cornillez-Ty, C.T., Liao, L., Yates, J.R., Kuhn, P., Buchmeier, M.J., 2009. Severe acute respiratory syndrome coronavirus nonstructural protein 2 interacts with a host protein complex involved in mitochondrial biogenesis and intracellular signaling. *J. Virol.* 83, 10314–10318. <https://doi.org/10.1128/jvi.00842-09>.
- Cui, J., Li, F., Shi, Z.L., 2019. Origin and evolution of pathogenic coronaviruses. *Nat. Rev. Microbiol.* <https://doi.org/10.1038/s41579-018-0118-9>.
- Dever, T.E., Dinman, J.D., Green, R., 2018. Translation elongation and recoding in eukaryotes. *Cold Spring Harb. Perspect. Biol.* 10, a032649. <https://doi.org/10.1101/cshperspect.a032649>.
- Dinman, J.D., 2019a. Slippery ribosomes prefer shapeshifting mRNAs. *Proc. Natl. Acad. Sci. U.S.A.* 201913074 <https://doi.org/10.1073/pnas.1913074116>.
- Dinman, J.D., 2019b. Scaring ribosomes shiftless. *Biochemistry* 58, 1831–1832. <https://doi.org/10.1021/acs.biochem.9b00162>.
- Dinman, J.D., 2018. Shapeshifting RNAs guide innate immunity. *J. Biol. Chem.* 293, 16125–16126. <https://doi.org/10.1074/jbc.H118.005799>.
- Dinman, J.D., Ruiz-Echevarria, M.J., Czaplinski, K., Peltz, S.W., 1997. Peptidyl transferase inhibitors have antiviral properties by altering programmed -1 ribosomal frameshifting efficiencies: development of model systems. *Proc. Natl. Acad. Sci. U.S.A.* 94, 6606–6611. <https://doi.org/10.1073/pnas.94.13.6606>.
- Dinman, J.D., Wickner, R.B., 1992. Ribosomal frameshifting efficiency and Gag/Gag-pol ratio are critical for yeast M1 double-stranded RNA virus propagation. *J. Virol.* 66, 3669–3676.
- Frank, J., 2017. Time-resolved cryo-electron microscopy: recent progress. *J. Struct. Biol.* 100, 303–306. <https://doi.org/10.1016/j.jsb.2017.06.005>.
- Galloux, M., Risso-Ballester, J., Richard, C.A., Fix, J., Rameix-Welti, M.A., Eléouët, J.F., 2020. Minimal elements required for the formation of respiratory syncytial virus cytoplasmic inclusion bodies in vivo and in vitro. *mBio* 11, 1–16. <https://doi.org/10.1128/mBio.01202-20>.
- Goss Kinzy, T., Harger, J.W., Carr-Schmid, A., Kwon, J., Shastry, M., Justice, M.C., Dinman, J.D., 2002. New targets for antivirals: the ribosomal A-site and the factors that interact with it. *Virology* 300, 60–70. <https://doi.org/10.1006/viro.2002.1567>.
- Hadfield, J., Brito, A.F., Swetnam, D.M., Vogels, C.B.F., Tokarz, R.E., Andersen, K.G., Smith, R.C., Bedford, T., Grubaugh, N.D., 2019. Twenty years of West Nile virus spread and evolution in the Americas visualized by Nextstrain. *PLoS Pathog.* <https://doi.org/10.1371/journal.ppat.1008042>.
- Halma, J.T.J., Ritchie, D.B., Cappellano, T.R., Neupane, K., Woodside, M.T., 2019. Complex dynamics under tension in a high-efficiency frameshift stimulatory structure. *Proc. Natl. Acad. Sci. U.S.A.* 116, 19500–19505.
- Halma, M.T.J., Ritchie, D.B., Woodside, M.T., 2020. Conformational Shannon entropy of mRNA structures from force spectroscopy measurements predicts the efficiency of -1 programmed ribosomal frameshift stimulation. *bioRxiv*. <https://doi.org/10.1101/2020.12.12.422522>, 2020.12.12.422522.
- Haniff, H.S., Tong, Y., Liu, X., Chen, J.L., Suresh, B.M., Andrews, R.J., Peterson, J.M., O'Leary, C.A., Benhamou, R.I., Moss, W.N., Disney, M.D., 2020. Targeting the SARS-CoV-2 RNA genome with small molecule binders and ribonuclease targeting chimera (RIBOTAC) degraders. *ACS Cent. Sci.* 2020, 1713–1721. <https://doi.org/10.1021/acscentsci.0c00984>.
- Harcourt, J., Tamin, A., Lu, X., Kamili, S., Sakthivel, S.K., Murray, J., Queen, K., Tao, Y., Paden, C.R., Zhang, J., Li, Y., Uehara, A., Wang, H., Goldsmith, C., Bullock, H.A., Wang, L., Whitaker, B., Lynch, B., Gautam, R., Schindewolf, C., Lokugamage, K.G., Scharton, D., Plante, J.A., Mirchandani, D., Widen, S.G., Narayanan, K., Makino, S., Ksiazek, T.G., Plante, K.S., Weaver, S.C., Lindstrom, S., Tong, S., Menachery, V.D., Thornburg, N.J., 2020. Severe acute respiratory syndrome coronavirus 2 from patient with coronavirus disease, United States. *Emerg. Infect. Dis.* 26, 1266–1273. <https://doi.org/10.3201/EID2606.200516>.
- Holmes, E.C., Dudas, G., Rambaut, A., Andersen, K.G., 2016. The evolution of Ebola virus: insights from the 2013–2016 epidemic. *Nature*. <https://doi.org/10.1038/nature19790>.
- Hu, H.-T., Cho, C.-P., Lin, Y.-H., Chang, K.-Y., 2016. A general strategy to inhibiting viral -1 frameshifting based on upstream attenuation duplex formation. *Nucleic Acids Res.* 44, 256–266. <https://doi.org/10.1093/nar/gkv1307>.
- Huston, N., Wan, H., Araujo Tavares, R. de C., Wilen, C., Pyle, A.M., 2020. Comprehensive in-vivo secondary structure of the SARS-CoV-2 genome reveals novel regulatory motifs and mechanisms. *bioRxiv Prepr. Serv. Biol.* <https://doi.org/10.1101/2020.07.10.197079>.
- Iserman, C., Roden, C.A., Boerneke, M.A., Sealton, R.S.G., McLaughlin, G.A., Jungreis, I., Fritch, E.J., Hou, Y.J., Ekena, J., Weidmann, C.A., Theesfeld, C.L., Kellis, M., Troyanskaya, O.G., Baric, R.S., Sheahan, T.P., Weeks, K.M., Gladfelter, A.S., 2020. Genomic RNA elements drive phase separation of the SARS-CoV-2 nucleocapsid. *Mol. Cell* 80 (6), 1078–1091.e6. <https://doi.org/10.1016/j.molcel.2020.11.041>. Epub 2020 Nov 27.
- Ishimaru, D., Plant, E.P., Sims, A.C., Yount, B.L., Roth, B.M., Eldho, N.V., Pérez-Alvarado, G.C., Armbruster, D.W., Baric, R.S., Dinman, J.D., Taylor, D.R., Hennig, M., Hennig, M., 2013. RNA dimerization plays a role in ribosomal frameshifting of the SARS coronavirus. *Nucleic Acids Res.* 41, 2594–2608. <https://doi.org/10.1093/nar/gks1361>.
- Jacks, T., Madhani, H.D., Masiraz, F.R., Varmus, H.E., 1988. Signals for ribosomal frameshifting in the Rous Sarcoma Virus gag-pol region. *Cell* 55, 447–458.
- Karacostas, V., Wolffe, E.J., Nagashima, K., Gonda, M.A., Moss, B., 1993. Overexpression of the HIV-1 gag-pol polyprotein results in intracellular activation of HIV-1 protease and inhibition of assembly and budding of virus-like particles. *Virology* 193, 661–671.
- Karesh, W.B., Dobson, A., Lloyd-Smith, J.O., Lubroth, J., Dixon, M.A., Bennett, M., Aldrich, S., Harrington, T., Formenty, P., Loh, E.H., MacHalaba, C.C., Thomas, M.J., Heymann, D.L., 2012. Ecology of zoonoses: natural and unnatural histories. *Lancet*. [https://doi.org/10.1016/S0140-6736\(12\)61678-X](https://doi.org/10.1016/S0140-6736(12)61678-X).
- Kelly, J.A., Olson, A.N., Neupane, K., Munshi, S., San Emeterio, J., Pollack, L., Woodside, M.T., Dinman, J.D., 2020. Structural and functional conservation of the programmed -1 ribosomal frameshift signal of SARS coronavirus 2 (SARS-CoV-2). *J. Biol. Chem.* <https://doi.org/10.1074/jbc.AC120.013449>.
- Kendra, J.A., de la Fuente, C., Brahm, A., Woodson, C., Bell, T.M., Chen, B., Khan, Y.A., Jacobs, J.L., Kehn-Hall, K., Dinman, J.D., 2017. Ablation of programmed -1 ribosomal frameshifting in Venezuelan equine encephalitis virus results in attenuated neuropathogenicity. *J. Virol.* 91 <https://doi.org/10.1128/JVI.01766-16> e01766-16.
- Kim, H.-K., Liu, F., Fei, J., Bustamante, C., Gonzalez, R.L., Tinoco, I., 2014. A frameshifting stimulatory stem loop destabilizes the hybrid state and impedes ribosomal translocation. *Proc. Natl. Acad. Sci. U. S. A.* 111, 5538–5543. <https://doi.org/10.1073/pnas.1403457111>.
- Lan, T., Allan, M., Malsick, L., Khandwala, S., Nyeo, S., Bathe, M., Griffiths, A., Routskin, S., 2020. Structure of the full SARS-CoV-2 RNA genome in infected cells. *bioRxiv* (29), 178343. <https://doi.org/10.1101/2020.06.29.178343>, 2020.06.
- Lei, J., Kusov, Y., Hilgenfeld, R., 2018. Nsp3 of coronaviruses: structures and functions of a large multi-domain protein. *Antivir. Res.* <https://doi.org/10.1016/j.antiviral.2017.11.001>.
- Maillard, P.V., Veen, A.G., Poirier, E.Z., Reis e Sousa, C., 2019. Slicing and dicing viruses: antiviral <sc>RNA</sc> interference in mammals. *EMBO J.* 38 <https://doi.org/10.15252/embj.2018100941>.
- Manfredonia, I., Nithin, C., Ponce-Salvatierra, A., Ghosh, P., Wiercki, T.K., Marinus, T., Ogando, N.S., Snijder, E.J., Van Hemert, M.J., Bujnicki, J.M., Incarnato, D., 2020. Genome-wide mapping of SARS-CoV-2 RNA structures identifies therapeutically-relevant elements. *Nucleic Acids Res.* <https://doi.org/10.1093/nar/gkaa1053>.
- Marczinke, B., Fisher, R., Vidakovic, M., Bloys, A.J., Brierley, I., 1998. Secondary structure and mutational analysis of the ribosomal frameshift signal of rous sarcoma virus. *J. Mol. Biol.* 284, 205–225.
- Mills, J.N., Gage, K.L., Khan, A.S., 2010. Potential influence of climate change on vector-borne and zoonotic diseases: a review and proposed research plan. *Environ. Health Perspect.* 118, 1507–1514. <https://doi.org/10.1289/ehp.0901389>.
- Moomau, C., Musalgaonkar, S., Khan, Y.A., Jones, J.E., Dinman, J.D., 2016. Structural and functional characterization of programmed ribosomal frameshift signals in West Nile virus strains reveals high structural plasticity among cis-acting RNA elements. *J. Biol. Chem.* 291, 15788–15795. <https://doi.org/10.1074/jbc.M116.735613>.
- Neuman, B.W., Angelini, M.M., Buchmeier, M.J., 2014. Does form meet function in the coronavirus replicative organelle? *Trends Microbiol.* <https://doi.org/10.1016/j.tim.2014.06.003>.
- Neupane, K., Munshi, S., Zhao, M., Ritchie, D.B., Ieperuma, S.M., Woodside, M.T., 2020. Anti-frameshifting ligand active against SARS coronavirus-2 is resistant to natural mutations of the frameshift-stimulatory pseudoknot. *J. Mol. Biol.* <https://doi.org/10.1016/j.jmb.2020.09.006>. PMID: PMC7483078.
- Noller, H.F., Yusupov, M.M., Yusupova, G.Z., Baucom, A., Cate, J.H., 2002. Translocation of tRNA during protein synthesis. *FEBS Lett.* 514, 11–16.
- Omar, S.I., Zhao, M., Sekar, R.V., Moghadam, S.A., Tuszyński, J.A., Woodside, M.T., 2020. Modeling the structure of the frameshift stimulatory pseudoknot in SARS-CoV-

- 2 reveals multiple possible conformers. *bioRxiv*. <https://doi.org/10.1101/2020.06.08.141150>, 2020.06.08.141150.
- Park, S.J., Kim, Y.G., Park, H.J., 2011. Identification of RNA pseudoknot-binding ligand that inhibits the -1 ribosomal frameshifting of SARS-coronavirus by structure-based virtual screening. *J. Am. Chem. Soc.* 133, 10094–10100.
- Paules, C.L., Marston, H.D., Fauci, A.S., 2020. Coronavirus infections—more than just the common cold. *JAMA, J. Am. Med. Assoc.* <https://doi.org/10.1001/jama.2020.0757>.
- Plant, E.P., Dinman, J.D., 2008. The role of programmed-1 ribosomal frameshifting in coronavirus propagation. *Front. Biosci.* 13, 4873–4881. <https://doi.org/10.2741/3046>.
- Plant, E.P., Dinman, J.D., 2005. Torsional restraint: a new twist on frameshifting pseudoknots. *Nucleic Acids Res.* 33, 1825–1833. <https://doi.org/10.1093/nar/gki329>.
- Plant, E.P., Jacobs, K.L.M., Harger, J.W., Meskauskas, A., Jacobs, J.L., Baxter, J.L., Petrov, A.N., Dinman, J.D., 2003. The 9-angstrom solution: how mRNA pseudoknots promote efficient programmed -1 ribosomal frameshifting. *RNA* 9, 168–174. <https://doi.org/10.1261/rna.2132503.or>.
- Plant, E.P., Pérez-Alvarado, G.C., Jacobs, J.L., Mukhopadhyay, B., Hennig, M., Dinman, J.D., 2005. A three-stemmed mRNA pseudoknot in the SARS coronavirus frameshift signal. *PLoS Biol.* 3, e172. <https://doi.org/10.1371/journal.pbio.0030172>.
- Plant, E.P., Rakauskaitė, R., Taylor, D.R., Dinman, J.D., 2010. Achieving a golden mean: mechanisms by which coronaviruses ensure synthesis of the correct stoichiometric ratios of viral proteins. *J. Virol.* 84, 4330–4340. <https://doi.org/10.1128/JVI.02480-09>.
- Plant, E.P., Sims, A.C., Baric, R.S., Dinman, J.D., Taylor, D.R., 2013. Altering SARS coronavirus frameshift efficiency affects genomic and subgenomic RNA production. *Viruses* 5, 279–294. <https://doi.org/10.3390/v5010279>.
- Rabl, J., Leibundgut, M., Ataie, S.F., Haag, A., Ban, N., 2011. Crystal structure of the eukaryotic 40S ribosomal subunit in complex with initiation factor 1. *Science* 331 (80), 730–736.
- Ramos, F.D., Carrasco, M., Doyle, T., Brierley, I., 2004. Programmed -1 ribosomal frameshifting in the SARS coronavirus. *Biochem. Soc. Trans.* 32, 1081–1083.
- Rangan, R., Zheludev, I.N., Hagey, R.J., Pham, E.A., Wayment-Steele, H.K., Glenn, J.S., Das, R., 2020. RNA genome conservation and secondary structure in SARS-CoV-2 and SARS-related viruses: a first look. *RNA* 26, 937–959. <https://doi.org/10.1261/rna.076141.120>.
- Ritchie, D.B., Cappellano, T.R., Tittle, C., Rezajoei, N., Rouleau, L., Sikkema, W.K., Woodside, M.T., 2017. Conformational Dynamics of the Frameshift Stimulatory Structure in HIV-1, vol. 117. *RNA*, 061655.
- Ritchie, D.B., Foster, D.A.N., Woodside, M.T., 2012. Programmed -1 frameshifting efficiency correlates with RNA pseudoknot conformational plasticity, not resistance to mechanical unfolding. *Proc. Natl. Acad. Sci. U.S.A.* 102, 16167–16172.
- Ritchie, D.B., Soong, J., Sikkema, W.K.A., Woodside, M.T., 2014. Anti-frameshifting ligand reduces the conformational plasticity of the SARS virus pseudoknot. *J. Am. Chem. Soc.* 136, 2196–2199. <https://doi.org/10.1021/ja410344b>.
- Rodnina, M.V., Fricke, R., Kuhn, L., Wintermeyer, W., 1995. Codon-dependent conformational change of elongation factor Tu preceding GTP hydrolysis on the ribosome. *EMBO J.* 14, 2613–2619.
- Rodnina, M.V., Korniy, N., Klimova, M., Karki, P., Peng, B.-Z., Senyushkina, T., Belardinelli, R., Maracci, C., Wohlgenuth, I., Samatova, E., Peske, F., 2019. Translational recoding: canonical translation mechanisms reinterpreted. *Nucleic Acids Res.* <https://doi.org/10.1093/nar/gkz783>.
- Ruijtenberg, S., Sonneveld, S., Cui, T.J., Logister, I., de Steenwinkel, D., Xiao, Y., MacRae, I.J., Joo, C., Tanenbaum, M.E., 2020. mRNA structural dynamics shape Argonaute-target interactions. *Nat. Struct. Mol. Biol.* 27, 790–801. <https://doi.org/10.1038/s41594-020-0461-1>.
- Ryder, S., Morgan, B., Massi, F., 2020. Analysis of rapidly emerging variants in structured regions of the SARS-CoV-2 genome. *bioRxiv Prepr. Serv. Biol.* <https://doi.org/10.1101/2020.05.27.120105>, 2020.05.27.120105.
- Sakar, L., Lee, K., Cannito, B., Gilmore, A., Campbell-Lendrum, D., 2004. Globalization and Infectious Diseases: A Review of the Linkages. World Health Organization. [http://www.who.int/tdr/publications/documents/seb\\_topic3.pdf](http://www.who.int/tdr/publications/documents/seb_topic3.pdf).
- Schubert, K., Karousis, E.D., Jomaa, A., Scaiola, A., Echeverria, B., Gurzeler, L.A., Leibundgut, M., Thiel, V., Mühlemann, O., Ban, N., 2020. SARS-CoV-2 Nsp1 binds the ribosomal mRNA channel to inhibit translation. *Nat. Struct. Mol. Biol.* 27, 959–966. <https://doi.org/10.1038/s41594-020-0511-8>.
- Somogyi, P., Jenner, A.J., Brierley, I.A., Inglis, S.C., 1993. Ribosomal pausing during translation of an RNA pseudoknot. *Mol. Cell Biol.* 13, 6931–6940.
- Su, M.C., Chang, C.T., Chu, C.H., Tsai, C.H., Chang, K.Y., 2005. An atypical RNA pseudoknot stimulator and an upstream attenuation signal for -1 ribosomal frameshifting of SARS coronavirus. *Nucleic Acids Res.* 33, 4265–4275.
- Sun, Y., Abriola, L., Surovtseva, Y.V., Lindenbach, B.D., Guo, J.U., 2020. Restriction of SARS-CoV-2 replication by targeting programmed -1 ribosomal frameshifting in vitro. *bioRxiv*. <https://doi.org/10.1101/2020.10.21.349225>, 2020.10.21.349225.
- Takayr, S., Hickerson, R.P., Noller, H.F., 2005. mRNA helicase activity of the ribosome. *Cell* 120, 49–58.
- Volpato, G., Fontefrancesco, M.F., Gruppiso, P., Zocchi, D.M., Pieroni, A., 2020. Baby pangolins on my plate: possible lessons to learn from the COVID-19 pandemic. *J. Ethnobiol. Ethnomed.* <https://doi.org/10.1186/s13002-020-00366-4>.
- Wacker, A., Weigand, J.E., Akabayov, S.R., Altincekic, N., Bains, J.K., Banijamali, E., Binas, O., Castillo-Martinez, J., Cetiner, E., Ceylan, B., Chiu, L.-Y., Davila-Calderon, J., Dhamotharan, K., Duchardt-Ferner, E., Ferner, J., Frydman, L., Fürtig, B., Gallego, J., Grün, J.T., Hacker, C., Haddad, C., Hähnke, M., Hengesbach, M., Hiller, F., Hohmann, K.F., Hymon, D., de Jesus, V., Jonker, H., Keller, H., Knezic, B., Landgraf, T., Löhr, F., Luo, L., Mertinkus, K.R., Muhs, C., Novakovic, M., Oxenfarth, A., Palomino-Schätzlein, M., Petzold, K., Peter, S.A., Pypfer, D.J., Qureshi, N.S., Riad, M., Richter, C., Saxena, K., Schamber, T., Scherf, T., Schlagmitweit, J., Schlundt, A., Schnieders, R., Schwalbe, H., Simba-Lahuasi, A., Sreeramulu, S., Stirmal, E., Sudakov, A., Tants, J.-N., Tolbert, B.S., Vögele, J., Weiß, L., Wirmir-Bartoschek, J., Wirtz Martin, M.A., Wöhrner, J., Zetzsche, H., 2020. Secondary structure determination of conserved SARS-CoV-2 RNA elements by NMR spectroscopy. *Nucleic Acids Res.* <https://doi.org/10.1093/nar/gkaa1013>.
- Wang, X., Xuan, Y., Han, Y., Ding, X., Ye, K., Yang, F., Gao, P., Goff, S.P., Gao, G., 2019. Regulation of HIV-1 gag-pol expression by shiftless, an inhibitor of programmed -1 ribosomal frameshifting. *Cell* 176, 625–635. <https://doi.org/10.1016/j.cell.2018.12.030> e14.
- Wang, Y., Grunewald, M., Perlman, S., 2020. Coronaviruses: an updated overview of their replication and pathogenesis. In: *Methods in Molecular Biology*. Humana Press Inc., pp. 1–29. [https://doi.org/10.1007/978-1-0716-0900-2\\_1](https://doi.org/10.1007/978-1-0716-0900-2_1).
- Weaver, S.C., Charlier, C., Vasilakis, N., Lecuit, M., 2018. Zika, Chikungunya, and other emerging vector-borne viral diseases. *Annu. Rev. Med.* 69, 395–408. <https://doi.org/10.1146/annurev-med-050715-105122>.
- Wong, A.C.P., Li, X., Lau, S.K.P., Woo, P.C.Y., 2019. Global epidemiology of bat coronaviruses. *Viruses*. <https://doi.org/10.3390/v11020174>.
- Wu, A., Peng, Y., Huang, B., Ding, X., Wang, X., Niu, P., Meng, J., Zhu, Z., Zhang, Z., Wang, J., Sheng, J., Quan, L., Xia, Z., Tan, W., Cheng, G., Jiang, T., 2020. Genome composition and divergence of the novel coronavirus (2019-nCoV) originating in China. *Cell Host Microbe* 27, 325–328. <https://doi.org/10.1016/j.chom.2020.02.001>.
- Xie, M., Chen, Q., 2020. Insight into 2019 novel coronavirus — an updated interim review and lessons from SARS-CoV and MERS-CoV. *Int. J. Infect. Dis.* <https://doi.org/10.1016/j.ijid.2020.03.071>.
- Yan, S., Wen, J.-D., Bustamante, C., Tinoco, I., 2015. Ribosome excursions during mRNA translocation mediate broad branching of frameshift pathways. *Cell* 160, 870–881. <https://doi.org/10.1016/j.cell.2015.02.003>.
- Yang, L., Zhong, Z., Tong, C., Jia, H., Liu, Y., Chen, G., 2018. Single-molecule mechanical folding and unfolding of RNA hairpins: effects of single A-U to A-C pair substitutions and single proton binding and implications for mRNA structure-induced -1 ribosomal frameshifting. *J. Am. Chem. Soc.* 140 <https://doi.org/10.1021/JACS.8B02970>.
- Zhang, K., Zheludev, I., Hagey, R., Wu, M.T.-P., Haslecker, R., Hou, Y., Kretschi, R., Pintilie, G., Rangan, R., Kladwang, W., Li, S., Pham, E., Bernardin-Souibgui, C., Baric, R., Sheahan, T., D'Souza, V., Glenn, J., Chiu, W., Das, R., 2020. Cryo-electron microscopy and exploratory antisense targeting of the 28-kDa frameshift stimulation element from the SARS-CoV-2 RNA genome. *bioRxiv Prepr. Serv. Biol.* <https://doi.org/10.1101/2020.07.18.209270>, 2020.07.18.209270.
- Zhang, X., Xu, X., Yang, Z., Burcke, A.J., Gates, K.S., Chen, S.J., Gu, L.Q., 2015. Mimicking ribosomal unfolding of RNA pseudoknot in a protein channel. *J. Am. Chem. Soc.* 137, 15742–15752. <https://doi.org/10.1021/jacs.5b07910>.
- Zhou, Y., Su, J.M., Samuel, C.E., Ma, D., 2019. Measles virus forms inclusion bodies with properties of liquid organelles. *J. Virol.* 93 <https://doi.org/10.1128/jvi.00948-19>.